

Original Research

# Gastrodin Prevents Neuronal Apoptosis and Improves Neurological Deficits in Traumatic Brain Injury Rats through PKA/CREB/Bcl2 Axis

Chenglong Sun<sup>1</sup>, Wenhao Zheng<sup>1</sup>, Linjie Wang<sup>2</sup>, Quan Du<sup>1,\*</sup>

<sup>1</sup>Department of Neurosurgery, Affiliated Hangzhou First People's Hospital, Zhejiang University School of Medicine, 310030 Hangzhou, Zhejiang, China

<sup>2</sup>The Fourth Clinical Medical College, Zhejiang Chinese Medical University, 310053 Hangzhou, Zhejiang, China

\*Correspondence: [duquan76@163.com](mailto:duquan76@163.com) (Quan Du)

Academic Editor: Antoni Camins

Submitted: 7 September 2022 Revised: 10 November 2022 Accepted: 15 November 2022 Published: 18 May 2023

## Abstract

**Background:** Gastrodin (Gas) exhibits anti-inflammatory properties against diseases associated with the central nervous system (CNS). This study aimed to investigate the potential neuroprotective role of Gas in traumatic brain injury (TBI). **Methods:** A rat TBI model was established in male adult Sprague-Dawley (SD) rats by controlled cortical impingement (CCI), and lipopolysaccharide (LPS) was applied to induce the activation of BV2 microglia and HT22 hippocampal neurons. Neurological deficits, motor function and brain water content were evaluated in TBI rats. TUNEL and Nissl's staining were applied to measure neuronal degeneration and apoptosis. Microglial activation, the mRNA and protein profiles of pro-inflammatory cytokines were tested by immunohistochemistry (IHC), quantitative reverse transcriptase-polymerase chain reaction (qRT-PCR) and enzyme-linked immunosorbent assay (ELISA), respectively. **Results:** Gas significantly reduced neurological deficits, cerebral edema, and neuronal apoptosis and improved motor function in TBI mice. In addition, Gas inactivated microglia and blocked the production of pro-inflammatory cytokines on the damaged side of the TBI rat brain. *In vitro*, Gas attenuated BV2 microglia inflammation and reduced HT22 hippocampal neuronal apoptosis. On the other hand, Gas activated the PKA/CREB/BDNF pathway both *in vivo* and *in vitro*. **Conclusions:** Gas blocks microglial activation-mediated inflammation through the PKA/CREB/BDNF pathway, thereby improving neurobehavioral function after TBI, which provides a potential therapeutic benefit for treating TBI.

**Keywords:** gastrodin; neurological protection; microglial activation; traumatic brain injury

## 1. Introduction

Traumatic brain injury (TBI) is the primary reason for long-term disability and death among young people, which imposes a significant economic and medical burden on society [1]. TBI can be divided into primary and secondary injuries. The initial damaging force can lead to primary brain injury, resulting in tissue destruction and deformation early after injury. Secondary injuries appear hours, days, or months after the primary injury and include inflammation, brain edema, blood-brain barrier (BBB) rupture, oxidative stress, excitotoxicity, and mitochondrial and metabolic dysfunction [2]. An estimated 10 million people are yearly affected by TBI, and mortality and morbidity are increasing each year, making it a global health challenge.

Inflammation is a critical factor in TBI, leading to extensive cell death and chronic tissue degeneration. Astrocytes, microglia, and central nervous system (CNS) cells are thought to be essential factors in triggering the inflammatory response after injury [3]. Microglia are the main cellular component of the innate immune system of the central nervous system and are the first line of defense in the event of injury or disease. In the injured brain, microglia activate and produce numerous pro-inflammatory and cytotoxic mediators that impede CNS repair and lead to neu-

ronal dysfunction and apoptosis [4]. Additionally, several studies have shown that inactivating microglia in TBI reduces the production of inflammatory cytokines, but the specific mechanism still needs further exploration [5–7]. Therefore, searching for pharmacological strategies to inhibit microglial status may be an effective way to minimize post-TBI brain damage and improve neurological function.

Gastrodin (Gas), a phenolic glycoside, is the dominating bioactive constituent of *Rhizoma Gastrodiae*. Since its identification in 1978, Gas has been found to have beneficial effects on the CNS through modulation of neurotransmitters, anti-oxidant and anti-inflammatory effects, and inhibition of microglial activation through the MAPK pathway [8]. It has been confirmed that Gas pretreatment reduces ischemia/reperfusion (I/R) injury-induced neurobehavioral deficits in rats, attenuates the size of cerebral infarction, reverses blood-brain barrier (BBB) injury and alleviates inflammation [9]. Besides, in the rat intracerebral hemorrhage (ICH) model, Gas distinctly improves brain edema and neurological deficits after ICH and represses oxidative stress and neuronal apoptosis in ICH rat brain tissues [10]. More importantly, Yao YY *et al.* [11] found that Gas abates the proliferation of BV2 microglia stimulated by lipopolysaccharide (LPS) and reduces the expression of



inflammatory cytokines in BV2 cells. The same findings are also obtained by Li JJ *et al.* [12]. Gas inactivates microglia, thereby reducing neuroinflammation. However, research on Gas therapy for TBI is limited. This paper aims to investigate the effect of Gas on inflammation after TBI and its related mechanisms and to provide a basis for the clinical practice of Gas in treating TBI.

## 2. Materials and Methods

### 2.1 Cell Culture and Treatment

BV2 microglia and HT22 hippocampal neurons were obtained from the Chinese Academy of Sciences (Shanghai, China). All cell lines were tested for mycoplasma and no mycoplasma contamination was observed. All cell lines were detected by Short Tandem Repeat (STR) test and all were detected correctly. Cells were maintained in DMEM with 10% FBS and 1% penicillin/streptomycin. The cell viability was examined periodically, and the medium was replaced every three days. The logarithmic growth phase cells were selected. BV2 microglia ( $5 \times 10^4$ ) and HT22 hippocampal neurons ( $5 \times 10^4$ ) were inoculated into 96-well plates and treated with LPS (1  $\mu\text{g/mL}$ ) for 24 hours with or without the treatment of 40  $\mu\text{M}$  Gas.

### 2.2 Animals

The animal test was authorized by the Experimental Animal Ethics Committee of Zhejiang University School of Medicine and implemented under strict supervision (EAECZUSM20210013). Forty adult male Sprague-Dawley (SD) rats (220–270 g) were purchased from the Institute of Experimental Animals of Wuhan University. Rats were placed in a temperature ( $23 \pm 2^\circ\text{C}$ ) and light controlled room.

### 2.3 The TBI Model

Rats were divided into sham, Gas, TBI, and TBI+Gas groups (10 rats in each group). The stereotactic impactor Impact One™ (Leica Biosystems, Deer Park, IL, USA) was applied to cause controlled cortical impingement (CCI) damage in rats [13]. The rats were immobilized in a stereotactic instrument and anesthetized with isoflurane through a nasal mask. The induction rate was 3%, and the maintenance rate was 2%. A midline incision was made in the skull. Unilateral craniectomy was carried out between Bregma and Lambda with a hand drill (5 mm in diameter). The rats were hit with a 4.0 mm stainless steel flat impactor tip. The conditions were as follows: stereotactic coordinates (AP:  $-2.26\text{ mm}$  and ML:  $+2.0\text{ mm}$ ), depth (0.65 mm), speed (4.0 m/s), residence time (200 ms), and angle ( $0.4^\circ$ ). After the injury, the bleeding was cleaned up, the incision was sutured, and the anesthesia was immediately removed. After the surgery, the rats were placed in cages on heating pads. The recovery of each rat was observed until they were standing on their four paws. The sham-operated rats underwent the same process as those with CCI injury, with-

out craniotomy and later hits. Rats in the Gas group and TBI+Gas group were intraperitoneally injected with Gas (100 mg/kg; Sigma, USA) one hour before CCI, once daily for seven days. In contrast, the sham and TBI groups were not treated.

### 2.4 The Brain Water Content

As previously stated [14], the rats were decapitated after the nerve injury was assessed. Their brains were harvested immediately at 3 and 7 days after the surgery. For craniotomy, a portion of the cerebral cortex was isolated (about 2 mm;  $200 \pm 20\text{ mg}$ ). Blood and cerebrospinal fluid were cleaned with filter paper. After the wet weight was measured with a digital scale, the sample was dried at  $100^\circ\text{C}$  for one day. Subsequently, the weight of each sample was determined. The brain water content =  $100\% \times (\text{wet weight} - \text{dry weight})/\text{dry weight}$ .

### 2.5 Rotarod Test

The Rotarod test was utilized to test motor coordination and balance [15,16]. Before CCI induction, train rats to hold on to the rotarod for 120 s at 10 rpm (adaptation phase). After the rat was accustomed to running on the stick, the speed was accelerated to 40 rpm for 300 s. The mean time to fall of the last three trials was recorded as the baseline latency. After CCI, rats were examined three times on days 1, 3, 7, 14 and 21, and the mean fall latency was recorded.

### 2.6 TdT-Mediated dUTP Nick end Labeling (TUNEL) Staining and Nissl Staining

TUNEL staining and Nissl staining were performed with the method of Wang H [17]. First, antigen-retrieved brain slices were incubated with a TUNEL reaction mix (Beyotime, China) for one hour at room temperature. After washing with phosphate buffered saline (PBS) for 20 min, the slides were incubated with DAPI for 5 min. Then, the sections were rinsed twice and observed with an inverted fluorescence microscope. ImageJ software was used to count TUNEL-positive cells. The number of apoptotic cells relative to DAPI was considered the apoptotic index. For Nissl staining, sections were stained in Nissl staining solution (Beyotime, China) for 5 min, washed with double distilled water, and mounted with Permunt. This photo was taken under an optical microscope. Neurons with visible nuclei and relatively intact cell morphology were counted by ImageJ (version 2, LOCI, University of Wisconsin, Madison, WI, USA) and Cellcounter software 1.0 (Ningbo Shunyu Technology, China).

### 2.7 Immunohistochemistry (IHC)

Rats were sacrificed under chloral hydrate anesthesia. The injured side brain tissue was taken, stored in 100 g/L paraformaldehyde solution, and fixed at room temperature for 24 hours. Cut the brain tissue into 3–4  $\mu\text{m}$  coronal sections and place in the oven for 4–6 h. Then, the sections

**Table 1. Primer sequences.**

| Target        | Forward (5'-3')           | Reverse (5'-3')        |
|---------------|---------------------------|------------------------|
| IL-1 $\beta$  | GGATGATGACGACCTGC         | CTTGTTGGCTTATGTTCTG    |
| IL-6          | TTTACCAGGCAAGTCTCCT       | AGACAGCCACTCACCTCTTC   |
| TNF- $\alpha$ | CTTATCTACTCCCAGGTTCTCTCAA | GAGACTCCTCCCAGGTACATGG |
| GAPDH         | GGGA GCCAAAAGGGTCAT       | GAGT CCTTCCACGATACCAA  |

were cleaned with PBS 3 times (2 min each time) and incubated with the rabbit anti-IBA1 antibody (1:500) in a 4 °C refrigerator overnight. After being washed, the sections were maintained with the horseradish peroxidase-labeled goat anti-rabbit IgG (1:800) at 37 °C for 2 hours. After the sections were washed, 3,3'-Diaminobenzidine (DAB) was utilized for color development. The control sections were incubated with PBS. Five fields of view on the damaged side of the section were taken without overlapping each other, and the IBA1-positive cells were calculated. The mean  $\pm$  standard deviation of the number of all positive cells in the sections of each group was taken as the immunohistochemical positive cell value of IBA1 in the damaged side brain tissue area of the group. The pathological alterations of brain tissues were reviewed under a microscope to confirm the degree of recovery.

## 2.8 Quantitative Reverse Transcriptase-Polymerase Chain Reaction (qRT-PCR)

Total RNA in tissues was extracted using the TRIzol reagent (Invitrogen, Waltham, MA, USA) according to the manufacturer's instructions. The RNA concentration and purity were determined with Nanodrop-spectrophotometer (Invitrogen, Waltham, MA, USA). Complementary DNA (cDNA) was synthesized from 1  $\mu$ g of total RNA with the PrimeScript-RT Kit (Takara, Japan). The qRT-PCR was performed on the ABI7300 Realtime PCR system (ABI, USA) using SYBR®Premix-Ex-Taq™ (Takara, Japan). The total volume of the PCR reaction was 30  $\mu$ L containing 300 ng of cDNA. The amplification was carried out with 10 min of initial denaturation at 95 °C, followed by 45 cycles of 95 °C for 10 seconds, 60 °C for 30 seconds, and 85 °C for 20 seconds. The GAPDH was set as the endogenous control of IL-1 $\beta$ , IL-6 and TNF- $\alpha$ . qRT-PCR was implemented three times. The primers were listed in Table 1.

## 2.9 Western Blotting (WB)

WB was carried out using the methods of predecessors [18].

The membranes were incubated with the primary antibodies (1:1000; Abcam, Waltham, MA, USA) overnight at 4 °C as follows: Bad (ab32445, Abcam, Waltham, MA, USA), Bax (ab32503, Abcam, Waltham, MA, USA), Bcl-2 (ab32124, Abcam, Waltham, MA, USA), iNOS (ab178945, Abcam, Waltham, MA, USA), TLR4 (ab13556, Abcam, Waltham, MA, USA), NF- $\kappa$ B (ab32536, Abcam, Waltham, MA, USA), p-NF- $\kappa$ B (ab76302, Abcam,

Waltham, MA, USA), PKA (ab32514, Abcam, Waltham, MA, USA), CREB1 (ab32515, Abcam, Waltham, MA, USA), p-CREB1 (ab32096, Abcam, Waltham, MA, USA), BDNF (ab203573, Abcam, Waltham, MA, USA), Bcl-2 (ab32124, Abcam, Waltham, MA, USA), and GAPDH (ab9485, Abcam, Waltham, MA, USA). Then, the membranes were rinsed with tris buffered saline with Tween 20 (TBST) twice and maintained with a fluorescein-labeled secondary antibody for 1 hour at RT. After being cleaned three times, the membranes were exposed to the enhanced chemiluminescence (ECL) chronotropic agent and imaged with a membrane scanner.

## 2.10 Enzyme-Linked Immunosorbent Assay (ELISA)

The interleukin (IL)-1 $\beta$ , IL-6, tumor necrosis factor- $\alpha$  (TNF- $\alpha$ ) and other cytokines were quantified by commercial ELISA kits (MultiSciences, Hangzhou, China) following the manufacturer's instructions [19].

## 2.11 Cell Counting Kit-8 (CCK-8) Assay

Cell viability was determined by CCK-8 assay. The cells were plated into 96-well plates at a density of  $1 \times 10^3$  cells per well and cultured for 24 hours. Each well was added 10  $\mu$ L of CCK-8 reagent (Dojindo Molecular Technologies, Kumamoto, Japan). After 1 hour of incubation at 37 °C, the optical density (OD) at 450 nm was determined with a spectrophotometer (Bio-Rad, CA, USA).

## 2.12 Flow Cytometry (FCM)

The cells were trypsinized and harvested by centrifugation at 1500 rpm for 3 min. The cell apoptosis was determined by the apoptosis detection kit (Shanghai Aladdin biological technology Co., Ltd). Briefly, the cells were washed with PBS twice and then incubated with 400  $\mu$ L of pre-cooled PBS. Subsequently, cells were added 10  $\mu$ L of AnnexinV-FITC and 5  $\mu$ L of PI. After incubation in the dark for 30 min at 4 °C, the cell apoptosis was determined by flow cytometry (BD, USA). The cells were gated with FSC-A vs. SSC-A, and four populations including Annexin V<sup>-</sup>/PI<sup>-</sup>, Annexin V<sup>+</sup>/PI<sup>-</sup>, Annexin V<sup>+</sup>/PI<sup>+</sup> and Annexin V<sup>-</sup>/PI<sup>+</sup> were gated with Annexin V FITC-A vs. PI-A. The proportion of apoptotic cells was determined.

## 2.13 Statistical Analysis

Statistical analysis was performed by SPSS17.0 statistical software (IBM SPSS, Chicago, IL, USA). One-way analysis of variance (ANOVA) was used to compare be-

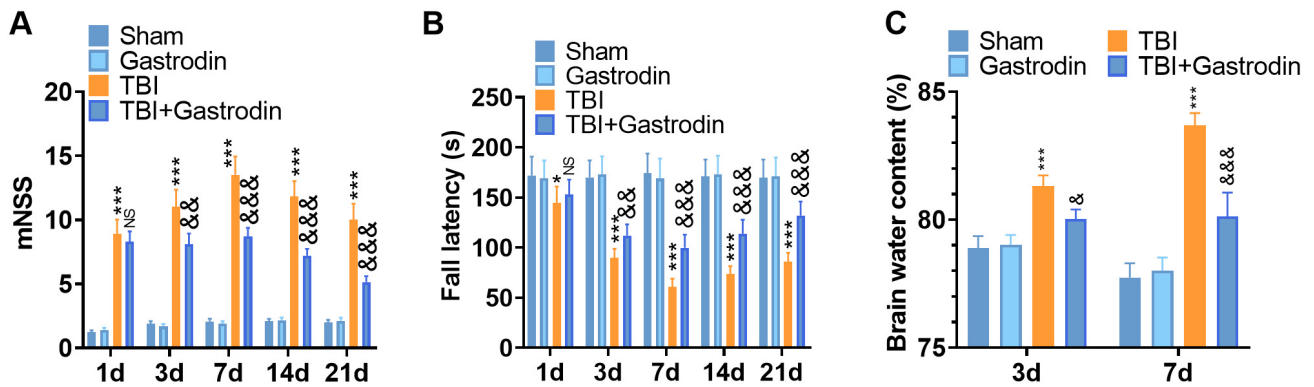


**Fig. 1. Gas reduced the neurological deficits and brain water content of TBI rats.** (A,B) The recovery of the nervous system was analyzed by mNSS (A), and Rota-rod (B) tests at 1, 3, 5, 7, 14 and 21 days after TBI. (C) The water content in the brain of TBI rats was assessed by the dry and wet method at 3, 7 and 21 days after TBI. \* $p < 0.05$ , \*\*\* $p < 0.001$  (vs. sham), NS  $p > 0.05$ , &  $p < 0.05$ , &&  $p < 0.01$ , &&&  $p < 0.001$  (vs. TBI).

tween groups. The measurement data were presented as mean  $\pm$  standard deviation (SD).  $p < 0.05$  indicated statistical significance.

### 3. Results

#### 3.1 Gas Reduced the Neurological Deficits and Brain Water Content of TBI Rats

To understand the effect of Gas (100 mg/kg) on the neurological function of TBI rats, we implemented a modified Neurological Severity Score (mNSS), rotarod test and the wet/dry method to test the neurological function, motor function and brain water content of TBI rats 1, 3, 7, 14 and 21 days after TBI. The findings demonstrated that mNSS in the sham and Gas group did not change at the corresponding time points (with a score of 1–3). Nevertheless, neurological function was seriously damaged by TBI. After the treatment of Gas, the mNSS of rats in the TBI+Gas group was significantly lower than that of the TBI group ( $p < 0.05$ , Fig. 1A). Meanwhile, the rotation performance of rats in the TBI+Gas group was better than that of the TBI group ( $p < 0.05$ , Fig. 1B). Additionally, compared with the sham group, the water content of brain tissues in the TBI group was dramatically higher ( $82.32 \pm 0.83\%$ ,  $p < 0.05$ ). Moreover, Gas treatment in the TBI model attenuated the water content ( $80.32 \pm 0.62\%$ ,  $p < 0.05$ , Fig. 1C).

#### 3.2 Gas Suppressed Neuronal Degeneration and Apoptosis after Brain Injury in Rats

Nissl and TUNEL staining were performed to verify neuronal apoptosis in the damaged side of the cerebral cortex of TBI rats. The results illustrated that the neurons in the sham group were clear and complete. In contrast, damaged neurons in the TBI group exhibited irregular cell bodies, enhanced crinkling and nuclear pigmentation, and increased TUNEL-positive cells. After the treatment of Gas, the neuronal loss and TUNEL-positive neurons decreased in the TBI group ( $p < 0.05$ , Fig. 2A–D). In addition, the

levels of apoptosis-related proteins in the damaged side of brain tissues of TBI rats were determined. The results revealed that the Bax and Bad expression was increased, and the Bcl-2 level was decreased in the TBI group compared with the sham group. After Gas treatment, the results were the opposite ( $p < 0.05$ , Fig. 2E). There was no significant difference between the TBI and the Gas groups. These results demonstrated that Gas reduced the apoptosis and degeneration of neurons in the brain of TBI rats.

#### 3.3 Gas Inhibited Microglial Inflammatory Responses in TBI Rats

First, IBA1-labeled microglia in the brain tissues of TBI rats were determined by IHC. The results indicated that IBA1 microglia were significantly increased in the TBI group compared with the sham group. However, the IBA1 microglia were reduced after Gas intervention ( $p < 0.05$ , Fig. 3A). The levels of IL-1 $\beta$ , IL-6 and TNF $\alpha$  in the brain tissues of TBI rats were measured by ELISA and qRT-PCR. Our results indicated that IL-1 $\beta$ , IL-6 and TNF $\alpha$  were up-regulated in the TBI group. However, they were down-regulated after Gas treatment ( $p < 0.05$ , Fig. 3B,C). WB results demonstrated that iNOS and TLR4 were upregulated, and the NF- $\kappa$ B phosphorylation was enhanced in the TBI group. After the Gas intervention, iNOS and TLR4 were down-regulated, and the NF- $\kappa$ B phosphorylation was decreased ( $p < 0.05$ , Fig. 3D). These results indicated that Gas attenuated microglial activation and inflammatory responses in TBI rats.

#### 3.4 Gas Activated the PKA/CREB/BDNF Expression

To explore the molecular mechanism of Gas *in vivo*, the effects of Gas on the PKA/CREB/BDNF pathway were determined. Our results indicated that the PKA level was decreased, the phosphorylation of CREB was inhibited, and Bcl2 was significantly downregulated in the TBI group compared with the sham group. However, Gas intervention



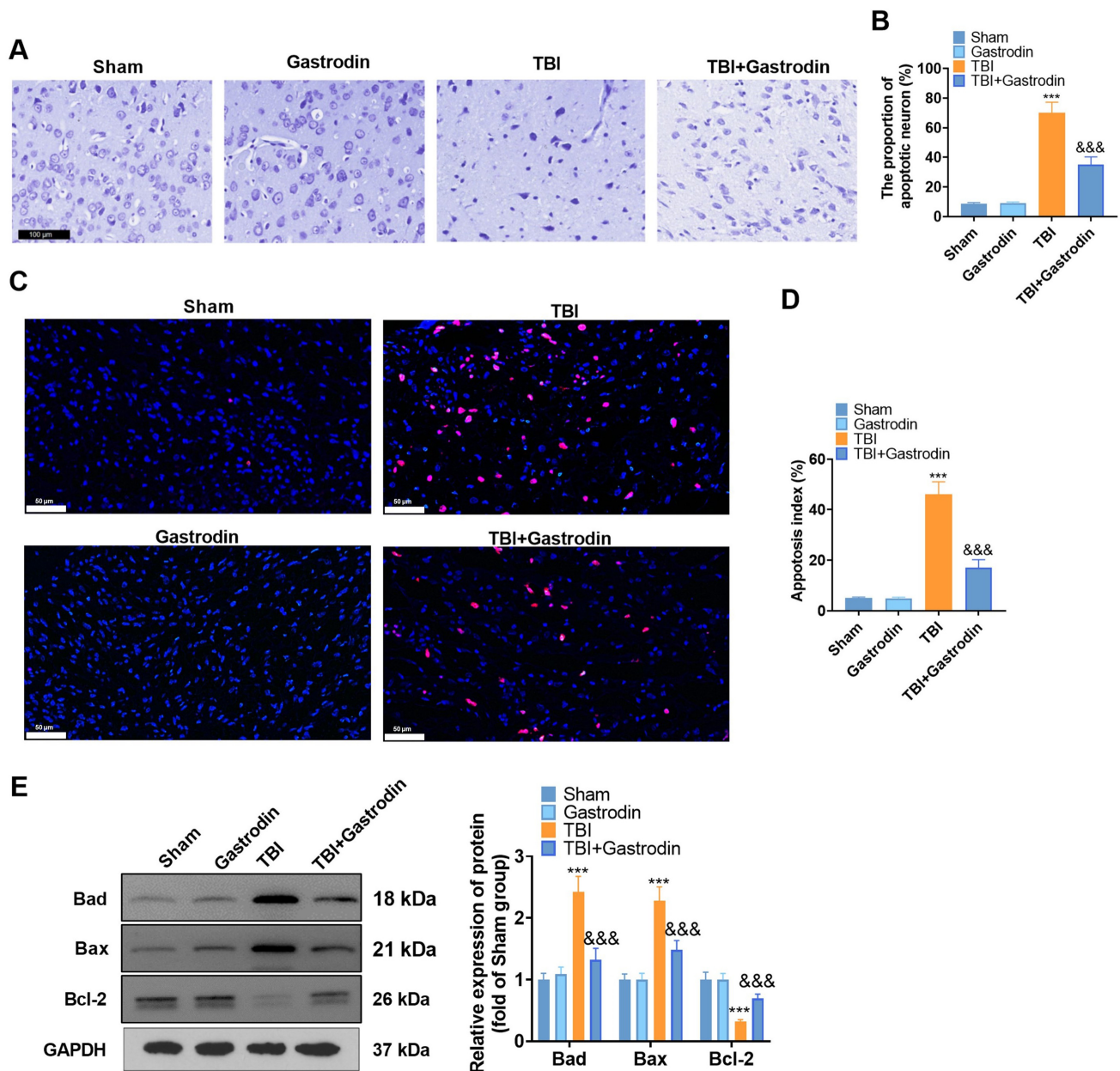


**Fig. 2. Gas inhibited neuronal degeneration and apoptosis after brain injury in rats.** (A,B) Representative photomicrograph (A) (scale = 100  $\mu\text{m}$ ) and quantification (B) of Nissl staining of the damaged side of the cortex of TBI rats on day 7. The red arrow indicates neuronal damage. (C,D) Representative micrograph (C) (scale = 50  $\mu\text{m}$ ) and quantification (D) of TUNEL staining in the damaged side of the cortex of TBI rats on day 7. (E) WB was carried out to test the profiles of apoptosis-related proteins in the damaged cortex of TBI rats on day 7. Data were expressed as mean  $\pm$  SD.  $n = 5$  for each group. \*\*\*  $p < 0.001$  (vs. sham), &&&  $p < 0.001$  (vs. TBI).

yielded opposite results ( $p < 0.05$ , Fig. 4A–D). These results confirmed that the mechanism of Gas might be related to the activation of the PKA/CREB/BDNF pathway.

### 3.5 Gas Attenuated LPS-Mediated Inflammatory Responses and Neuronal Apoptosis in BV2 Microglia

Inflammatory responses are the main pathological mechanism of brain injury. Therefore, the influence of Gas (40  $\mu\text{M}$ ) on inflammatory cytokines in LPS-treated BV2 microglia was determined. The IL-1 $\beta$ , IL-6 and TNF-

$\alpha$  were augmented in LPS-treated BV2 microglia. However, levels of IL-1 $\beta$ , IL-6 and TNF- $\alpha$  in BV2 microglia were dramatically reduced after Gas intervention ( $p < 0.05$ , Fig. 5A,B). WB results further confirmed that the levels of iNOS and TLR4 were strengthened, and the phosphorylation of NF- $\kappa\text{B}$  was elevated in the LPS group compared with the control group. However, after Gas intervention, the expression of iNOS and TLR4 was impeded, and the phosphorylation of NF- $\kappa\text{B}$  declined ( $p < 0.05$ , Fig. 5C). Additionally, the effects of Gas on neurons were evaluated.

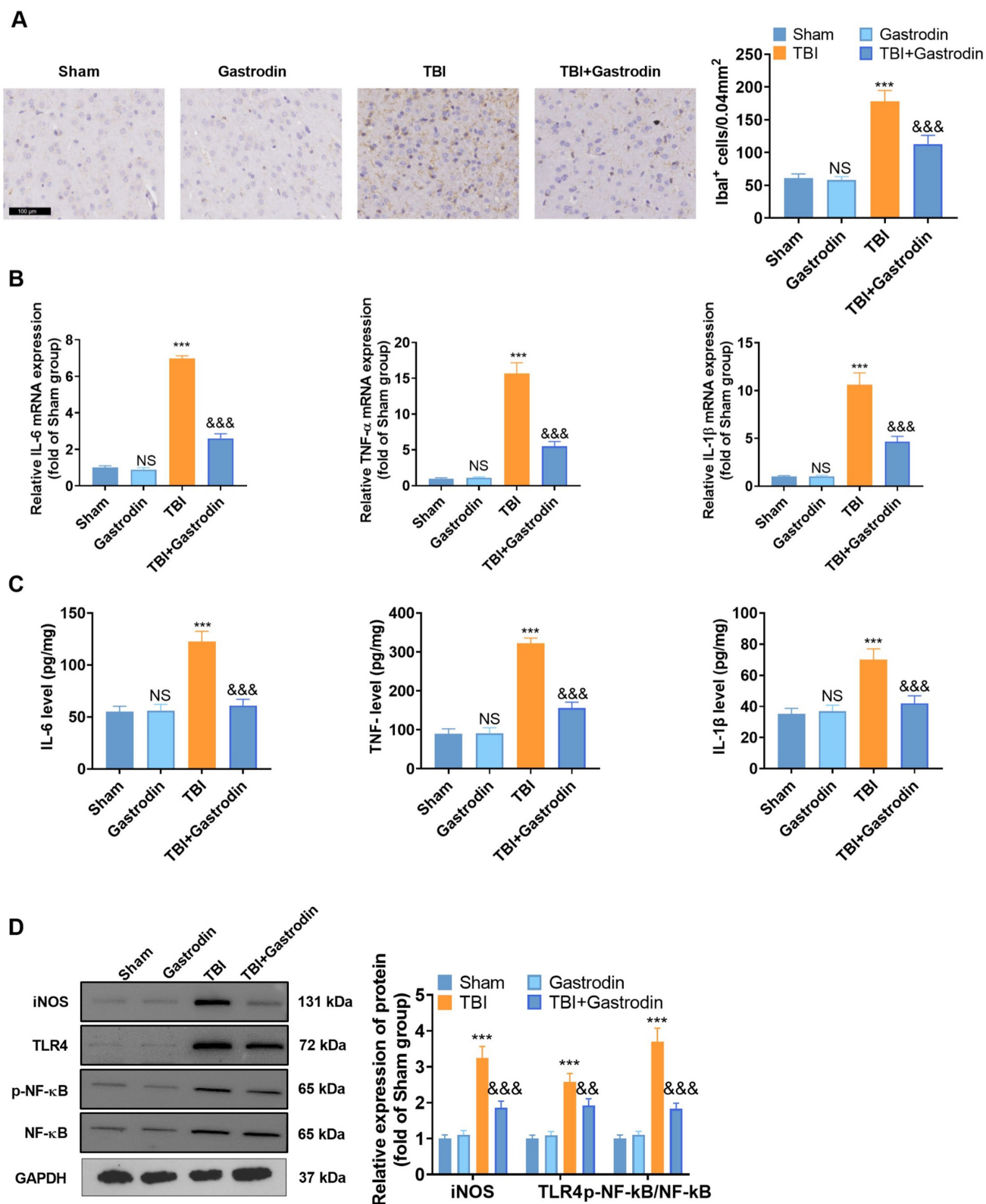


**Fig. 3. Gas repressed microglia-mediated inflammations in TBI rats.** (A) IHC was utilized to check the representative images and quantification of IBA1-positive cells in the damaged side of the cortex of TBI rats on day 7, with a scale of 100  $\mu\text{m}$ . (B,C) qRT-PCR (B) and ELISA (C) were applied to measure the expression of inflammatory factors in the damaged side of the cortex of TBI rats on day 7. (D) WB was conducted to monitor the levels of inflammatory proteins in the damaged side of the cortex of TBI rats on day 7. Data were expressed as mean  $\pm$  SD.  $n = 5$  for each group. NS  $p > 0.05$ , \*\*\*  $p < 0.001$  (vs. sham), &&  $p < 0.01$ , &&&  $p < 0.001$  (vs. TBI).

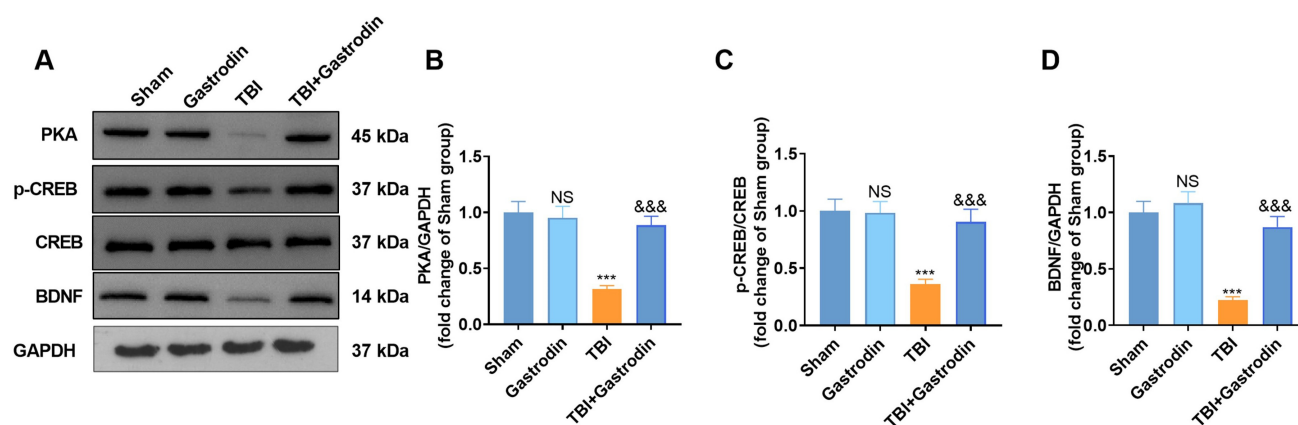


**Fig. 4. Gas activated the expression of PKA/CREB1/Bcl2.** (A–D) WB was utilized to test the PKA expression, the CREB phosphorylation, and the BDNF profile in the damaged side of the cortex of TBI rats on day 7. NS  $p > 0.05$ , \*\*\*  $p < 0.001$  (vs. sham), &&&  $p < 0.001$  (vs. TBI).

CCK-8 and FCM were utilized to determine cell viability and apoptosis. The results demonstrated that LPS treatment attenuated cell viability and increased cell apoptosis, while Gas treatment increased cell viability ( $p < 0.05$ , Fig. 5D) and reduced cell apoptosis ( $p < 0.05$ , Fig. 5E). Furthermore, Gas treatment suppressed the expression of apoptotic proteins ( $p < 0.05$ , Fig. 5F). These findings confirmed that Gas alleviated LPS-induced microglial inflammation and hippocampal neuronal damage.

### 3.6 Inhibiting the PKA/CREB/BDNF Pathway Weakened the Anti-Inflammatory and Anti-Apoptotic Effects of Gas on Cells

The effects of Gas *in vitro* have been determined. First, the PKA/CREB/BDNF pathway expression in LPS-treated BV2 microglia and HT22 hippocampal neurons was evaluated. The results confirmed that PKA was downregulated, the phosphorylation of CREB was reduced, and the expression of BDNF was significantly attenuated in the LPS group compared with the control group ( $p < 0.05$ , Fig. 6A,B). Therefore, the PKA/CREB/BDNF pathway was abnormally expressed in LPS-treated cells. Accordingly, BV2 microglia and HT22 hippocampal neurons were treated with the PKA inhibitors H89 (10  $\mu$ M) and Gas (40  $\mu$ M) and exposed them to LPS for 24 hours. The results confirmed that H89 treatment weakened the effects of Gas and enhanced inflammatory cytokines and inflammatory proteins in BV2 microglia ( $p < 0.05$ , Fig. 6C–E), declined the viability of HT22 hippocampal neurons ( $p < 0.05$ , Fig. 6F), and enhanced the apoptosis ( $p < 0.05$ , Fig. 6G,H). Furthermore, the LPS+H89+Gas treatment resulted in reduced PKA expression and downregulated phosphorylation of CREB and BDNF expression ( $p < 0.05$ , Fig. 6I). These findings demonstrated that inhibiting the PKA/CREB/BDNF pathway weakened the anti-inflammatory and anti-apoptotic effects of Gas *in vitro*.

## 4. Discussion

TBI is the cause of various neurological and cognitive deficits as well as psychosocial dysfunction. The incidence of TBI is in the millions every year and is increasing globally [20]. Although many promising neuroprotective therapeutic options have emerged from pre-clinical research primarily targeting lesions, they can still not be applied clinically [21]. Therefore, the development of effective drugs for the treatment of TBI is crucial. In this study, we explored the neuroprotective effects of Gas in a rat model of TBI and assessed the potential function of the PKA/CREB/BDNF pathway. The findings suggest that Gas exerts neuroprotective effects by activating the PKA/CREB/BDNF pathway.

Gastrodin (Gas; 4-hydroxybenzyl alcohol 4-O- $\beta$ -D-glucoside), a phenolic glucoside extracted from *Gastrodia elata*, exerts anti-oxidant, anti-inflammatory and anti-apoptotic activities in a variety of cells [22]. Pharmacokinetics showed that Gas could penetrate the blood and cerebrospinal fluid barrier [23]. Gas exerts not only anti-inflammatory, anti-oxidative stress and anti-apoptotic functions in cerebral ischemia [24,25], I/R [26] and Parkinson's disease (PD) [27] but also prevents neuronal apoptosis. It also regulates microglial activation and reduces microglia-mediated neuroinflammation [28,29]. In this study, we found that Gas improved the motor function of TBI rats by inactivating microglia in the injured brain tissue of TBI rats and preventing the production of pro-inflammatory cytokines, thereby improving neurological function loss, brain function loss after TBI Edema and neuronal apoptosis.

Cyclic adenosine monophosphate (cAMP), the first and second messenger identified, contributes to cell signaling and regulates various physiological and pathological processes. cAMP mainly regulates the transcription of multiple target genes through protein kinase A (PKA) and its downstream effectors, such as cAMP response ele-



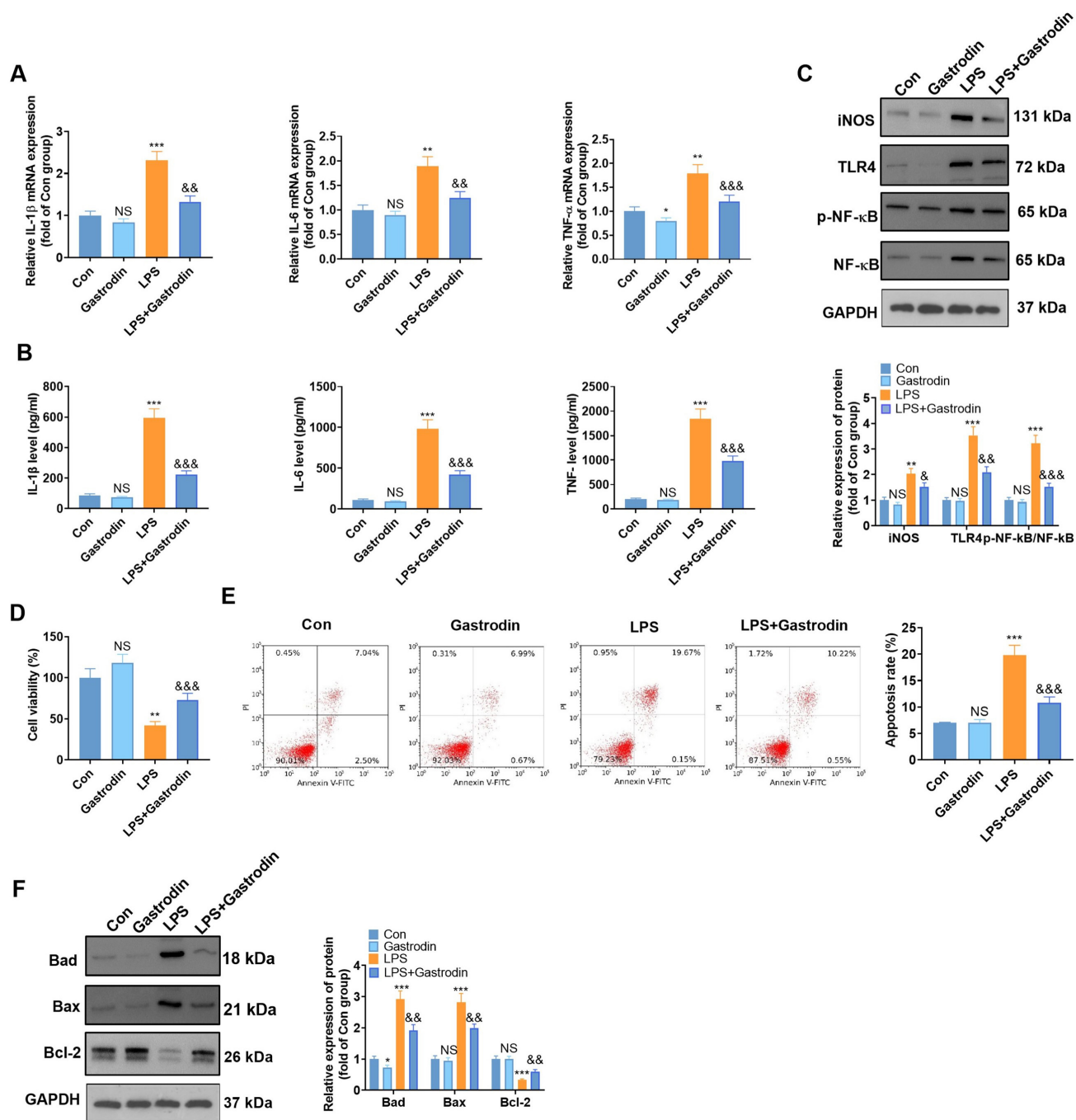


**Fig. 5.** Gas attenuated LPS-mediated inflammatory responses and neuronal apoptosis in BV2 microglia (suggestion: in row E, it would be better to use a bold or larger font to make the labels easy to read). BV2 microglia and HT22 hippocampal neurons were treated with LPS (1 g/mL) for 24 hours with or without Gas (40  $\mu$ M). (A,B) qRT-PCR (A) and ELISA (B) were employed to assay the expression of inflammatory cytokines in BV2 microglia. (C) WB was conducted to monitor the profiles of inflammatory proteins in BV2 microglia. (D) The effect of Gas on the viability of HT22 hippocampal neurons was analyzed by CCK-8. (E,F) FCM (E) and WB (F) were utilized to assess the impact of Gas on HT22 hippocampal neuronal apoptosis. Data were expressed as mean  $\pm$  SD.  $n = 5$  for each group. NS  $p > 0.05$ , \*  $p < 0.05$ , \*\*  $p < 0.01$ , \*\*\*  $p < 0.001$  (vs. Con), &  $p < 0.05$ , &&  $p < 0.01$ , &&&  $p < 0.001$  (vs. LPS).

ment binding protein (CREB) [30]. Previous studies have shown that drugs can reduce LPS-induced inflammatory cytokine production by modulating the cAMP-PKA pathway in BV2 cells [31]. For example, Morin suppressed LPS-stimulated microglia inflammation by upregulating

the PKA/CREB pathway [32]. BHDPC induces phosphorylation of PKA and CREB to suppress neuroinflammation in LPS-activated BV2 microglia and promote M2 polarization of microglia [33]. Furthermore, after TBI, the cAMP/PKA/CREB pathway is downregulated, while phos-



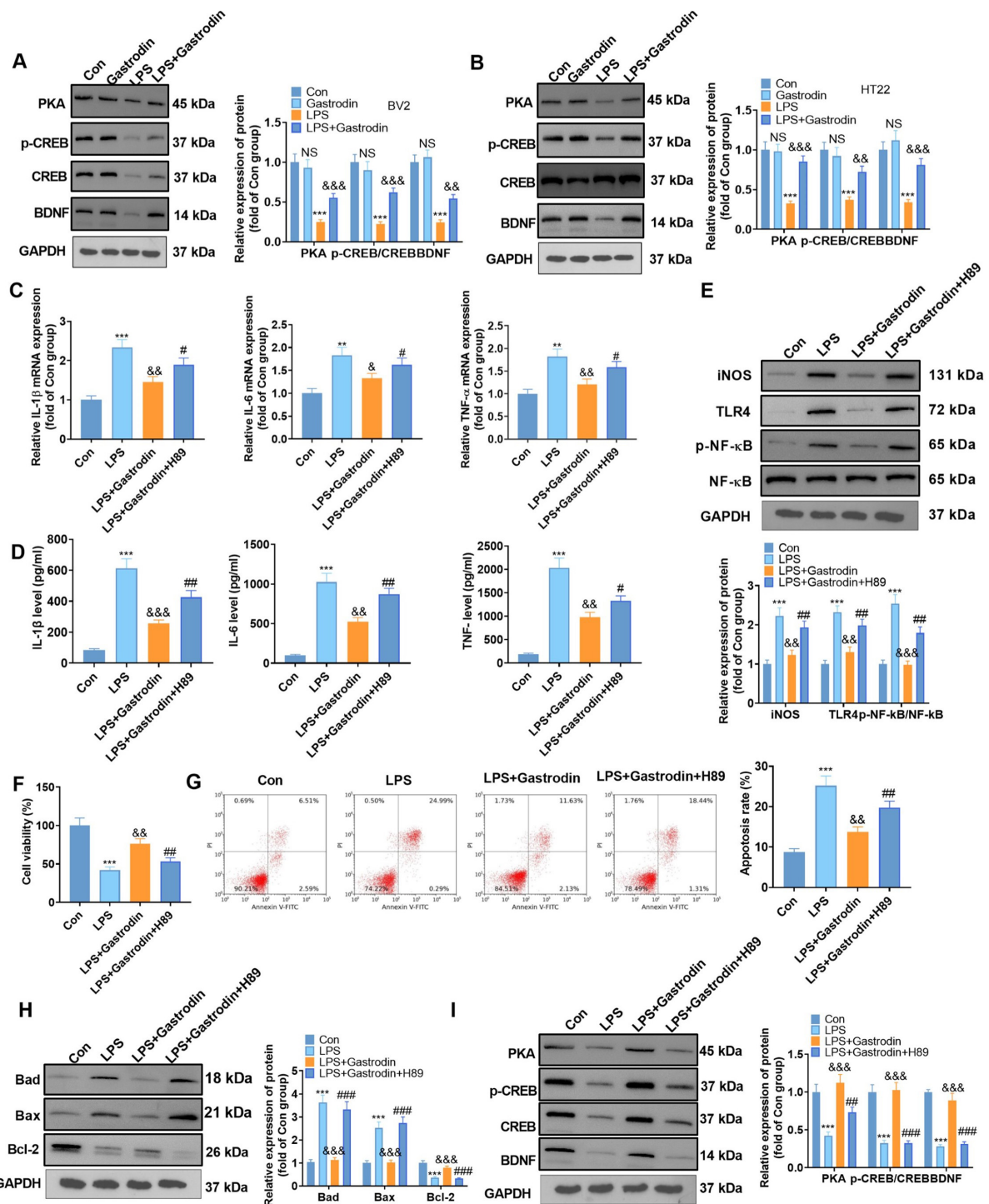


**Fig. 6. Inhibiting the PKA/CREB/BDNF pathway weakened the anti-inflammatory and anti-apoptotic effects of Gas on cells (suggestion: for row G, please refer to the suggestion for Fig. 5 row E).** (A,B) WB was employed to measure the PKA expression, CREB phosphorylation, and the BDNF profile in BV2 microglia and HT22 hippocampal neurons. (C,D) qRT-PCR (C) and ELISA (D) were applied to define the expression of inflammatory cytokines in BV2 microglia treated with H89 (10  $\mu$ M) and Gas. (E) The profiles of inflammatory proteins in BV2 microglia treated with H89 (10  $\mu$ M) and Gas were determined by WB. (F) CCK-8 was utilized to measure the effect of H89 (10  $\mu$ M) and Gas on the viability of HT22 hippocampal neurons. (G,H) FCM (G) and WB (H) were employed to verify the effect of H89 (10  $\mu$ M) and Gas on the apoptosis of HT22 hippocampal neurons. (I) The PKA/CREB/BDNF pathway expression in BV2 microglia treated with H89 (10  $\mu$ M) and Gas (40  $\mu$ M) was monitored by WB. Data were expressed as mean  $\pm$  SD.  $n = 5$  for each group. NS  $p > 0.05$ , \*\*  $p < 0.01$ , \*\*\*  $p < 0.001$  (vs. Con), &  $p < 0.05$ , &&  $p < 0.01$ , &&&  $p < 0.001$  (vs. LPS), #  $p < 0.05$ , ##  $p < 0.01$ , ###  $p < 0.001$  (vs. LPS+Gas).

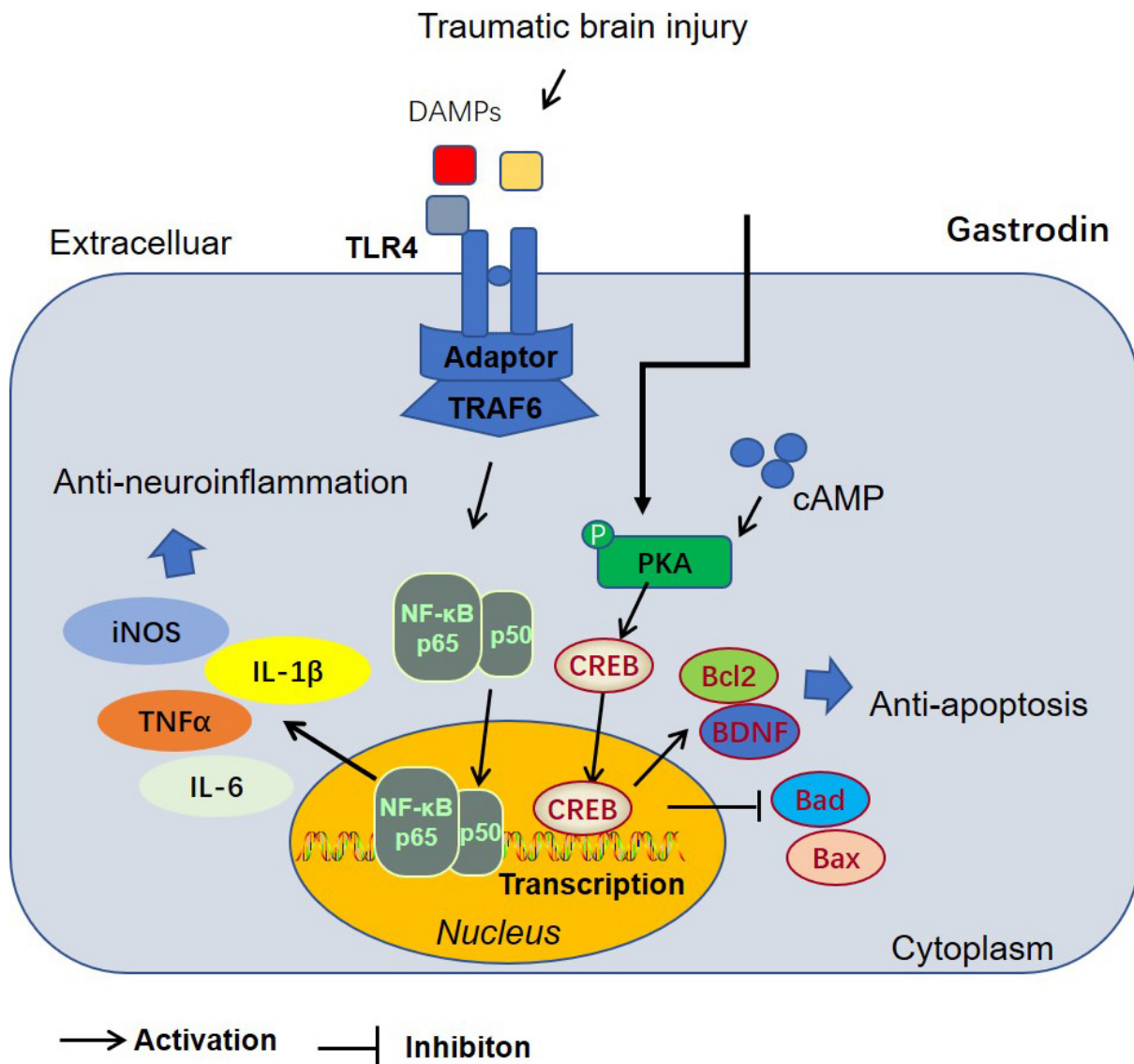


Fig. 7. The mechanism's diagram of Gas-mediated anti-apoptosis and anti-neuroinflammation via inhibiting the PKA/CREB1/Bcl2 pathway.

phodiesterase 4 activates CREB to improve cognitive impairment [34]. In this study, we found that Gas activates the PKA/CREB pathway in a rat model of TBI. Moreover, inhibition of the PKA/CREB pathway reversed Gas-mediated anti-inflammatory and anti-apoptotic effects. These results suggest that Gas protects against TBI-mediated nerve injury by activating the PKA/CREB pathway.

The protein family of B-cell lymphoma 2 (Bcl-2) is an important factor in the apoptotic pathway. The Bcl-2 family members mainly regulate apoptosis, and abnormal expression of Bcl-2 is associated with multiple diseases, including cancer, neurodegenerative diseases, local ischemia and autoimmune diseases [35]. Bcl2 is the target of CREB. A previous study demonstrated that inhibiting equilibrative nucleoside transporter 1 suppressed neuronal apoptosis and ameliorated neurological impairment through activation of cAMP/PKA/CREB pathway [36]. In ischemic brain injury,

propofol increases the contents of cleaved caspase-3 and Bax in rat hippocampal neurons by suppressing the activity of cAMP-dependent proteins and Bcl-2 [37]. Moreover, BDNF, as a neurotrophin, has been confirmed as a vital cytokine involved in synaptic transmission and long-term potentiation (LTP) in the hippocampus and other brain regions [38], and it also protects neurons from apoptosis in acute brain injury [39–41]. Therefore, we investigated the expression and role of the PKA/CREB/BDNF axis in TBI. The results demonstrated that Bcl2 and BDNF were down-regulated in the brain tissues of TBI rats, LPS-induced BV2 microglia and HT22 hippocampal neurons. In contrast, the Gas enhanced the expression of Bcl2 and BDNF, while inhibition of the PKA/CREB pathway by H89 weakened Bcl2 and BDNF levels. These results confirmed that Gas eases TBI by activating PKA/CREB/BDNF pathway.

This study contained limitations, and our results must be further validated in clinical applications. Currently, there is only the optimal model of TBI *in vivo*, and there is no excellent stimulation method to completely simulate the occurrence of TBI *in vitro*. This study employed LPS-mediated chemical brain injury to mimic this process. When TBI occurs, the human environment changes dramatically, and microglia polarize into one of two distinct phenotypes: M1 and M2. M1 microglia play a role in promoting the development of inflammation. Within injured tissue, microglia exist in various states of activation and retain the ability to alter their functional phenotype during inflammatory responses. When an injury occurs, microglia polarize towards a pro-inflammatory (M1) phenotype, produce pro-inflammatory cytokines such as TNF- $\alpha$ , interleukins (IL-1 $\beta$ , IL-12), present antigens, and express high levels of inducible nitric oxide synthase (iNOS) for NO production. In microglia, TLR-4/NF- $\kappa$ B is a traditional transcription factor activated by LPS and regulates the expression of most M1 phenotypic genes encoding pro-inflammatory cytokines (Fig. 7). Establishing efficient and accurate *in vitro* models of TBI in the future is crucial for studying TBI mechanisms and treatments.

## 5. Conclusions

In conclusion, our results indicated that Gas improves neural function and reduces neuronal apoptosis in TBI rats by targeting PKA/CREB/BDNF, suggesting that Gas is a new potential therapeutic approach for TBI treatment. To our knowledge, this is the first report on the role of Gas in TBI.

## Availability of Data and Materials

The datasets used and/or analyzed during the current study are available from the corresponding author on reasonable request.

## Author Contributions

CS, WZ and QD designed the research study. CS and WZ performed the research. LW analyzed the data. All authors contributed to editorial changes in the manuscript. All authors read and approved the final manuscript. All authors have participated sufficiently in the work and agreed to be accountable for all aspects of the work.

## Ethics Approval and Consent to Participate

The animal test was authorized by the Experimental Animal Ethics Committee of Zhejiang University School of Medicine and implemented under strict supervision (EAECZUSM20210013).

## Acknowledgment

Not applicable.

## Funding

This research was supported by the Medical Health Science and Technology Project of the Zhejiang Provincial Health Commission (2021KY229).

## Conflict of Interest

The authors declare no conflict of interest.

## References

- [1] Hackenberg K, Unterberg A. Traumatic brain injury. *Der Nervenarzt*. 2016; 87: 203–214; quiz 215–216. (In German)
- [2] Kaur P, Sharma S. Recent Advances in Pathophysiology of Traumatic Brain Injury. *Current Neuropharmacology*. 2018; 16: 1224–1238.
- [3] Karve IP, Taylor JM, Crack PJ. The contribution of astrocytes and microglia to traumatic brain injury. *British Journal of Pharmacology*. 2016; 173: 692–702.
- [4] Loane DJ, Kumar A. Microglia in the TBI brain: The good, the bad, and the dysregulated. *Experimental Neurology*. 2016; 275: 316–327.
- [5] Chen M, Chen Q, Tao T. Tanshinone IIA Promotes M2 Microglia by ER $\beta$ /IL-10 Pathway and Attenuates Neuronal Loss in Mouse TBI Model. *Neuropsychiatric Disease and Treatment*. 2020; 16: 3239–3250.
- [6] Kumar A, Henry RJ, Stoica BA, Loane DJ, Abulwerdi G, Bhat SA, *et al.* Neutral Sphingomyelinase Inhibition Alleviates LPS-Induced Microglia Activation and Neuroinflammation after Experimental Traumatic Brain Injury. *The Journal of Pharmacology and Experimental Therapeutics*. 2019; 368: 338–352.
- [7] Ju S, Xu C, Wang G, Zhang L. VEGF-C Induces Alternative Activation of Microglia to Promote Recovery from Traumatic Brain Injury. *Journal of Alzheimer's Disease*. 2019; 68: 1687–1697.
- [8] Liu Y, Gao J, Peng M, Meng H, Ma H, Cai P, *et al.* A Review on Central Nervous System Effects of Gastrodin. *Frontiers in Pharmacology*. 2018; 9: 24.
- [9] Li S, Bian L, Fu X, Ai Q, Sui Y, Zhang A, *et al.* Gastrodin pretreatment alleviates rat brain injury caused by cerebral ischemic-reperfusion. *Brain Research*. 2019; 1712: 207–216.
- [10] Liu XC, Wu CZ, Hu XF, Wang TL, Jin XP, Ke SF, *et al.* Gastrodin Attenuates Neuronal Apoptosis and Neurological Deficits after Experimental Intracerebral Hemorrhage. *Journal of Stroke and Cerebrovascular Diseases*. 2020; 29: 104483.
- [11] Yao YY, Bian LG, Yang P, Sui Y, Li R, Chen YL, *et al.* Gastrodin attenuates proliferation and inflammatory responses in activated microglia through Wnt/ $\beta$ -catenin signaling pathway. *Brain Research*. 2019; 1717: 190–203.
- [12] Li JJ, Liu SJ, Liu XY, Ling EA. Herbal Compounds with Special Reference to Gastrodin as Potential Therapeutic Agents for Microglia Mediated Neuroinflammation. *Current Medicinal Chemistry*. 2018; 25: 5958–5974.
- [13] Garg C, Seo JH, Ramachandran J, Loh JM, Calderon F, Contreras JE. Trovafloxacin attenuates neuroinflammation and improves outcome after traumatic brain injury in mice. *Journal of Neuroinflammation*. 2018; 15: 42.
- [14] Espirito Santo SG, Monte MG, Polegato BF, Barbisan LF, Romualdo GR. Protective Effects of Omega-3 Supplementation against Doxorubicin-Induced Deleterious Effects on the Liver and Kidneys of Rats. *Molecules*. 2023; 28: 3004.
- [15] Zhang M, Cui Z, Cui H, Cao Y, Zhong C, Wang Y. Astaxanthin alleviates cerebral edema by modulating NKCC1 and AQP4 expression after traumatic brain injury in mice. *BMC Neuroscience*. 2016; 17: 60.

- [16] Chen G, Zhang S, Shi J, Ai J, Qi M, Hang C. Simvastatin reduces secondary brain injury caused by cortical contusion in rats: possible involvement of TLR4/NF-kappaB pathway. *Experimental Neurology*. 2009; 216: 398–406.
- [17] Wang H, Zhou XM, Wu LY, Liu GJ, Xu WD, Zhang XS, *et al.* Aucubin alleviates oxidative stress and inflammation via Nrf2-mediated signaling activity in experimental traumatic brain injury. *Journal of Neuroinflammation*. 2020; 17: 188.
- [18] Liu Y, Zhang R, Yan K, Chen F, Huang W, Lv B, *et al.* Mesenchymal stem cells inhibit lipopolysaccharide-induced inflammatory responses of BV2 microglial cells through TSG-6. *Journal of Neuroinflammation*. 2014; 11: 135.
- [19] He GY, Zhao CH, Wu DG, Cheng H, Sun LA, Zhang DL, *et al.* S100A8 Promotes Inflammation via Toll-Like Receptor 4 After Experimental Traumatic Brain Injury. *Frontiers in Neuroscience*. 2021; 14: 616559.
- [20] Pavlovic D, Pekic S, Stojanovic M, Popovic V. Traumatic brain injury: neuropathological, neurocognitive and neurobehavioral sequelae. *Pituitary*. 2019; 22: 270–282.
- [21] Xiong Y, Zhang Y, Mahmood A, Chopp M. Investigational agents for treatment of traumatic brain injury. *Expert Opinion on Investigational Drugs*. 2015; 24: 743–760.
- [22] de Oliveira MR, Brasil FB, Fürstenau CR. Evaluation of the Mitochondria-Related Redox and Bioenergetics Effects of Gastrodin in SH-SY5Y Cells Exposed to Hydrogen Peroxide. *Journal of Molecular Neuroscience*. 2018; 64: 242–251.
- [23] Wang Q, Chen G, Zeng S. Distribution and metabolism of gastrodin in rat brain. *Journal of Pharmaceutical and Biomedical Analysis*. 2008; 46: 399–404.
- [24] Peng Z, Wang S, Chen G, Cai M, Liu R, Deng J, *et al.* Gastrodin alleviates cerebral ischemic damage in mice by improving antioxidant and anti-inflammation activities and inhibiting apoptosis pathway. *Neurochemical Research*. 2015; 40: 661–673.
- [25] Zhang HS, Liu MF, Ji XY, Jiang CR, Li ZL, OuYang B. Gastrodin combined with rhynchophylline inhibits cerebral ischaemia-induced inflammasome activation via upregulating miR-21-5p and miR-331-5p. *Life Sciences*. 2019; 239: 116935.
- [26] Zhou Y, Chen J, Yao Z, Gu X. Gastrodin ameliorates Concanavalin A-induced acute hepatitis via the IL6/JAK2/STAT3 pathway. *Immunopharmacol Immunotoxicol*. 2022; 44: 925–934.
- [27] Kumar H, Kim IS, More SV, Kim BW, Bahk YY, Choi DK. Gastrodin protects apoptotic dopaminergic neurons in a toxin-induced Parkinson's disease model. *Evidence-based Complementary and Alternative Medicine*. 2013; 2013: 514095.
- [28] Liu SJ, Liu XY, Li JH, Guo J, Li F, Gui Y, *et al.* Gastrodin attenuates microglia activation through renin-angiotensin system and Sirtuin3 pathway. *Neurochemistry International*. 2018; 120: 49–63.
- [29] Guo J, Zhang XLN, Bao ZR, Yang XK, Li LS, Zi Y, *et al.* Gastrodin Regulates the Notch Signaling Pathway and Sirt3 in Activated Microglia in Cerebral Hypoxic-Ischemia Neonatal Rats and in Activated BV-2 Microglia. *Neuromolecular Medicine*. 2021; 23: 348–362.
- [30] Zhang H, Kong Q, Wang J, Jiang Y, Hua H. Complex roles of cAMP-PKA-CREB signaling in cancer. *Experimental Hematology & Oncology*. 2020; 9: 32.
- [31] Sun J, Qian P, Kang Y, Dai HB, Wang FZ, Wang HY, *et al.* Adrenomedullin 2 attenuates LPS-induced inflammation in microglia cells by receptor-mediated cAMP-PKA pathway. *Neuropeptides*. 2021; 85: 102109.
- [32] Jung JS, Choi MJ, Lee YY, Moon BI, Park JS, Kim HS. Suppression of Lipopolysaccharide-Induced Neuroinflammation by Morin via MAPK, PI3K/Akt, and PKA/HO-1 Signaling Pathway Modulation. *Journal of Agricultural and Food Chemistry*. 2017; 65: 373–382.
- [33] Li C, Chen T, Zhou H, Feng Y, Hoi MPM, Ma D, *et al.* BHDPC Is a Novel Neuroprotectant That Provides Anti-neuroinflammatory and Neuroprotective Effects by Inactivating NF-κB and Activating PKA/CREB. *Frontiers in Pharmacology*. 2018; 9: 614.
- [34] Titus DJ, Sakurai A, Kang Y, Furones C, Jergova S, Santos R, *et al.* Phosphodiesterase inhibition rescues chronic cognitive deficits induced by traumatic brain injury. *The Journal of Neuroscience*. 2013; 33: 5216–5226.
- [35] Siddiqui WA, Ahad A, Ahsan H. The mystery of BCL2 family: Bcl-2 proteins and apoptosis: an update. *Archives of Toxicology*. 2015; 89: 289–317.
- [36] Zhang D, Jin W, Liu H, Liang T, Peng Y, Zhang J, *et al.* ENT1 inhibition attenuates apoptosis by activation of cAMP/pCREB/Bcl2 pathway after MCAO in rats. *Experimental Neurology*. 2020; 331: 113362.
- [37] Guan R, Lv J, Xiao F, Tu Y, Xie Y, Li L. Potential role of the cAMP/PKA/CREB signalling pathway in hypoxic preconditioning and effect on propofol induced neurotoxicity in the hippocampus of neonatal rats. *Molecular Medicine Reports*. 2019; 20: 1837–1845.
- [38] Leal G, Comprido D, Duarte CB. BDNF-induced local protein synthesis and synaptic plasticity. *Neuropharmacology*. 2014; 76: 639–656.
- [39] Kowiański P, Lietzau G, Czuba E, Waśkow M, Steliga A, Moryś J. BDNF: A Key Factor with Multipotent Impact on Brain Signaling and Synaptic Plasticity. *Cellular and Molecular Neurobiology*. 2018; 38: 579–593.
- [40] Gustafsson D, Klang A, Thams S, Rostami E. The Role of BDNF in Experimental and Clinical Traumatic Brain Injury. *International Journal of Molecular Sciences*. 2021; 22: 3582.
- [41] Wang Z, Zheng Y, Zheng M, Zhong J, Ma F, Zhou B, *et al.* Neurogenic Niche Conversion Strategy Induces Migration and Functional Neuronal Differentiation of Neural Precursor Cells Following Brain Injury. *Stem Cells and Development*. 2020; 29: 235–248.